Optical study of Cs_2ZnI_4

D. P. Billesbach and F. G. Ullman
Department of Electrical Engineering, University of Nebraska–Lincoln, Lincoln, Nebraska 68588-0511
(Received 2 December 1991; revised manuscript received 23 March 1992)

The relative linear birefringence of Cs_2ZnI_4 was measured along all orthorhombic *Pnam* axes with use of the rotating-analyzer method. These measurements showed three distinct phase transitions at 120, 109, and 94 K and another possible phase transition near 101 K. The transition at 94 K showed definite hysteresis (≈ 1 K), which indicates that it was a first-order transition. No hysteresis was observed at either of the transitions at 109 and 120 K. The shapes of these transitions, however, indicate that the one at 120 K was second order, and the one at 109 K was first order in nature. Rough Brewster's-angle measurements were made which yielded a crude estimate of the average index of refraction of between 1.77 and 1.80. X-ray-diffraction measurements were also made to confirm our identification of the crystals grown and to identify the crystal orientation. These measurements yielded accurate values for the axial lengths of the room-temperature structure that are in very good agreement with previous measurements.

I. INTRODUCTION

In past years there has been much interest in the class of compounds that have the β-K_2SO_4 structure at some temperature.[1] The most studied member of this group has been K_2SeO_4 (Ref. 1) (other members of this subfamily include Rb_2ZnCl_4, Rb_2ZnBr_4, and K_2ZnCl_4). These compounds have a high-temperature (sometimes virtual) hexagonal $P6_3/mmc$ parent phase, which on cooling, transforms to the prototypic orthorhombic *Pnam* structure. Upon further cooling the crystal transforms to a structurally modulated incommensurate phase.[1] The modulation can be described by a wave vector $q_i=\frac{1}{3}(1-\delta)a^*$. At lower temperatures this "near tripling" becomes exact and the structure locks in to an improper ferroelectric phase that has tripled along the old modulation direction and belongs to the orthorhombic space group $Pna2_1$.[1] In some cases these crystals undergo further phase transitions, usually to monoclinic structures.

There is a second subfamily of A_2BX_4 compounds that likewise show the *Pnam* structure. Like the K_2SeO_4 subfamily, these compounds undergo a structural phase transition to an incommensurately modulated phase. The difference, however, is in the size of the modulation wave vector q_i. Whereas q_i for K_2SeO_4 is near $\frac{1}{3}a^*$, q_i for this second family (typified by Cs_2CdBr_4) is much closer to the zone center ($q_i\approx 0.15a^*$).[2–4] This, in turn, changes the character of the lock-in transition. The lock-in transition is no longer to a cell-tripled ferroelectric, orthorhombic phase, but instead is a zone-center transition to a monoclinic, ferroelastic phase with $P2_1/n$ symmetry.

It is not clear to which subfamily Cs_2ZnI_4 should belong because there is little information available about Cs_2ZnI_4. In 1971, Scaife determined the room-temperature axial lengths for Cs_2ZnI_4 and showed that the structure at liquid-nitrogen temperature differed from the one observed at room temperature.[5] Later, in 1981, Gesi performed dielectric measurements which showed three phase transitions at 110, 102, and 90 K.[6] These measurements also showed that none of the four phases were ferroelectric. Most recently, Aleksandrova *et al.*, on the basis of NMR measurements on Cs_2ZnI_4, proposed a sequence of space groups for the four known phases.[7]

It has been shown that linear birefringence can be a sensitive indicator of structural phase transitions.[8] Also, the shapes of the birefringence anomalies can give insight into the nature of the transitions. For these reasons we have measured the relative birefringence along all three crystallographic axes of Cs_2ZnI_4.

II. SYNTHESIS

Our attempts at growing Cs_2ZnI_4 by the methods of various workers yielded confusing results. Crystals were grown by slow evaporation at room temperature (from partially covered beakers) of an aqueous solution with a stoichiometric mixture of CsI and ZnI_2. Initial investigations of these slightly yellowish rectangular crystals showed no phase transitions and slightly larger lattice constants than previously reported[5] with some large unidentifiable diffraction peaks. A full x-ray structural analysis later showed that these crystals were actually the related compound Cs_3ZnI_5.[9]

By using a nonstoichiometric mixture (about 500% excess ZnI_2) and dark growing conditions (to avoid aqueous photochemical reactions), we succeeded in producing the desired compound, Cs_2ZnI_4. The crystals produced were thin, flat, rectangular plates. The polarized Raman-spectra and x-ray-diffraction data showed that the large face was perpendicular to the *Pnam b* axis.

III. X-RAY-DIFFRACTION ANALYSIS

The lattice constants of the crystals were determined by x-ray powder diffraction. The system used was a Rigaku D-MAX B system with a water-cooled copper anode tube and a graphite monochromator. The sample

to be analyzed was crushed with a mortar and pestle, and packed in an aluminum powder holder. The sample was then mounted in a θ-2θ goniometer. θ scans were done with a step size of 0.05°. The peaks in the resulting diffraction pattern were matched to particular (h,k,l) planes by comparison with a calculated pattern for the assumed lattice constants. Then, using 26 of these peaks, a best-fit set of lattice constants was determined. The fit was excellent, with no significant peak unaccounted for. The lattice constants calculated are listed in Table I along with the lattice constants determined by Scaife.[5]

Finally, as a reference system, a large crystal was cut and polished along its axes as determined by crossed polarizer extinctions. A complete set of polarized Raman spectra were then taken of this sample at room temperature. The marked crystal was then sent out to be x-ray oriented.[9] Subsequent crystals could then be oriented in house by comparison of their polarized Raman spectra to this set of standards.

IV. BREWSTER'S-ANGLE MEASUREMENTS

Crude Brewster's-angle measurements were made using a polarized He-Ne laser as a light source ($\lambda=632.8$ nm) and a visual spectroscope table as a goniometer. A thin polished sample was mounted on the prism table of the spectroscope such that the crystal surface was on the rotational axis of the table and the polarization of the laser was directed along a crystal axis. The table was rotated so that the beam was reflected back along its incident direction (autocollimated) to reference the table with the incident-light direction. The table was then rotated while observing the intensity of the reflected spot. When the spot intensity was at a minimum, the table position was noted, and the Brewster's-angle was calculated by taking the difference between the minimum-intensity position and the incident-beam position. Five repetitions were used to calculate an average angle. The crystal was then rotated by 90° about the incident direction and the measurements were repeated. Because of the scatter in the data obtained from this crude experiment, we were not able to determine the individual indices of refraction for the different lattice directions. We were only able to determine that the average index of refraction of Cs_2ZnI_4 was between 1.77 and 1.80 at a wavelength of 632.8 nm.

V. BIREFRINGENCE

A. Instrumentation

The relative birefringence was measured with the rotating-analyzer method of Wood and Glazer.[10] The apparatus used is shown schematically in Fig. 1. Light from a Uniphase model 1305P 5-mW linearly polarized He-Ne laser passed through a Babinet-Soleil compensator. This allowed complete control of the polarization state of the light incident on the sample. In this experiment we usually used circularly polarized light. The beam exiting the sample first struck a thin glass plate (at near-normal incidence), and a small fraction was reflected to a Coherent Optics model 90 power meter. This allowed us to monitor the total transmitted intensity (regardless of its polarization state). The majority of the beam passed through the glass plate and passed through the rotating analyzer. This was simply a synchronous chopper mechanism with a two-slot reference blade. The main chopper blade was replaced with a sheet of linear polaroid. The light that passed through the rotating analyzer was detected by a silicon photovoltaic cell. The resulting electrical signal was then lock-in detected at twice the rotation frequency of the chopper.

The sample was cut so that the incident light propagated along one of the orthorhombic axes. The sample thicknesses used ranged from 0.3 to 1.5 mm depending on the propagation direction of the light. The crystal was mounted in a liquid-nitrogen-cooled exchange gas cryostat of our own design and construction.[11] The temperature of the sample was measured with a platinum resistance thermometer connected to a $5\frac{1}{2}$ digit multimeter. A coil of nichrome wire wound around the cryostat tip and a voltage-controlled current source were used to control the sample temperature.

All of the various signals were read and recorded by a Digital Equipment Corp. LSI-11 microcomputer. The computer was also programmed to vary the temperature of the sample either up or down at a preset rate (usually about 0.3 K/min).

As shown in the Appendix [Eq. (A11)], there were three components of the intensity leaving the rotating analyzer. The lock-in amplifier only responded to components proportional to some function of 2ω or, in this case, the in-phase and quadrature components. By adjusting the relative orientations of the crystal and rotating analyzer (to set α to zero), there were two possible outputs of the lock-in amplifier. Depending on the phase

TABLE I. Lattice constants of Cs_2ZnI_4 as determined from x-ray diffraction.

Axis	Scaife[a]	This work
a	10.84 Å	10.827±0.006 Å
b	14.45 Å	14.450±0.008 Å
c	8.29 Å	8.289±0.005 Å

[a]Reference 5.

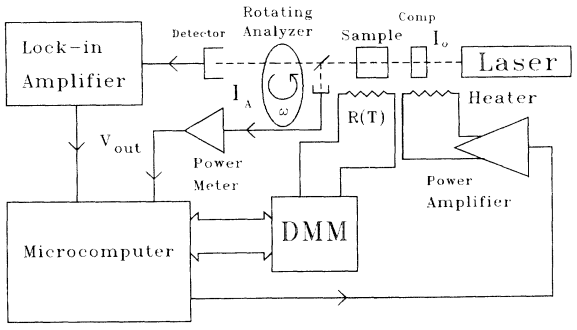

FIG. 1. Experimental setup.

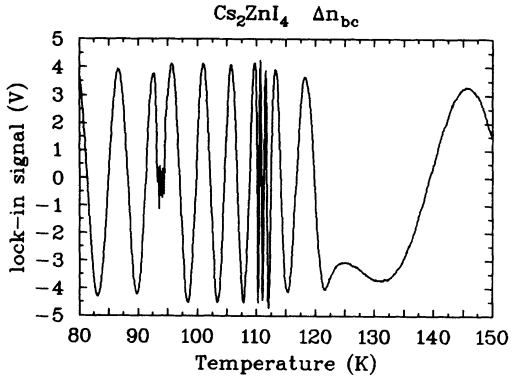

FIG. 2. Typical lock-in output vs temperature.

setting, the outputs were either

$$V_{\text{in-phase}} \propto t_x t_y A \cos[\phi+\delta(T)] , \quad (1)$$

for a lock-in phase of 0°, or

$$V_{\text{quad}} \propto \tfrac{1}{2}(t_x^2-t_y^2 A^2) , \quad (2)$$

for a lock-in phase of 90°. Obviously, since we were interested in the temperature-dependent birefringence [contained in the $\delta(T)$ term], we chose the 0° or in-phase setting. In practice, the phase α could not be set to zero with an accuracy greater than about ±5°. Measurements of the quadrature signal, however, showed that the component $(t_x^2-t_y^2A^2)$ was small, making the phase error negligible.

The phase shift $\delta(T)$ that was extracted from $V_{\text{in-phase}}$ is related to the birefringence $\Delta n_{xy}(T)$ by

$$\delta(T)=\frac{2\pi\Delta n_{xy}(T)d}{\lambda} , \quad (3)$$

where d is the crystal thickness (in the propagation direction), λ is the laser wavelength, and $\Delta n_{xy}(T)$ is the temperature-dependent birefringence.

B. Results

The output of the lock-in amplifier from a typical birefringence scan is shown in Fig. 2. Phase-transition anomalies are clearly seen near 120, 110, and 94 K. Figures 3–5 show the three components of the relative

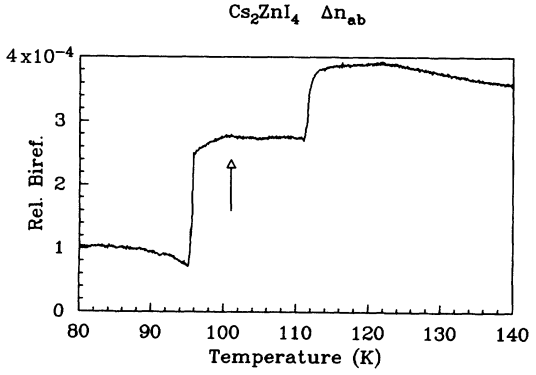

FIG. 3. Relative birefringence Δn_{ab}. The arrow indicates a probable phase transition near 101 K.

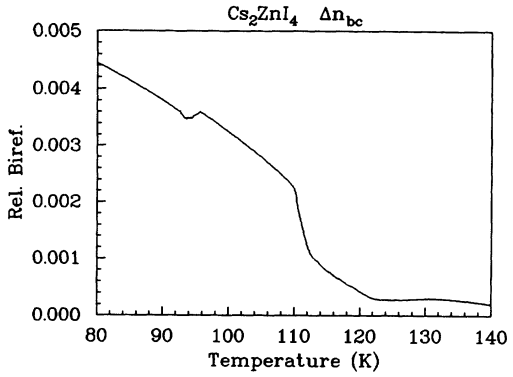

FIG. 4. Relative birefringence Δn_{bc}.

birefringence as extracted from the lock-in amplifier signals. The anomalies at 110 and 94 K are steplike, and the one at 120 K is continuous in temperature. This suggests that the transition at 120 K is of second order and the transitions at 110 and 94 K are of first order. Figure 6 shows these data plotted on a common birefringence scale. This shows that the variations in the components Δn_{ac} and Δn_{bc} are of roughly equal magnitude, but the Δn_{ab} variation component is much smaller. This implies that the c-axis component of the refractive index undergoes the largest changes with temperature.

Close examination of Fig. 3 shows a very small and apparently second-order anomaly near 101 K. This anomaly was seen in several scans and may correspond to the dielectric anomaly observed by Gesi at 102 K.[6]

Table II lists the average transition temperatures from several measurements. It should be noted that (depending on the sample and the heating or cooling rate) the transition at 94 K showed about 1 K of hysteresis.

The upper trace in Fig. 7 shows the lock-in output of a very slow (about 0.2 K/min) heating scan of the Δn_{ac} birefringence component. The lower trace shows a fast-cooling (about 12 K/min) run (the temperature scale on the fast-cooling scan was shifted to correct approximately for the temperature gradient set up between the crystal and thermometer). The two curves are essentially identical except for the region below 94 K. In the slow-heating run (and in similar slow-cooling runs), the region below 94 K is nearly flat, indicating a nearly constant

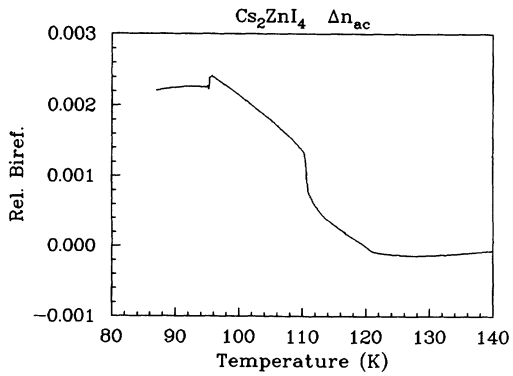

FIG. 5. Relative birefringence Δn_{ac}.

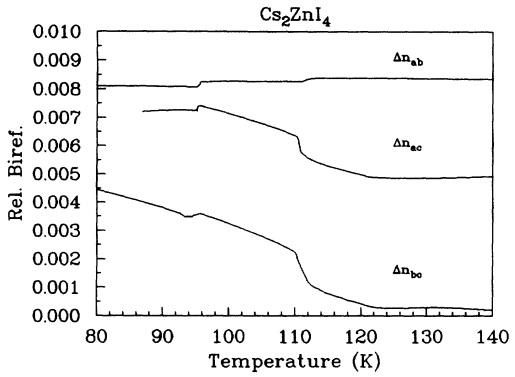

FIG. 6. Relative birefringence for all directions, plotted to a common scale.

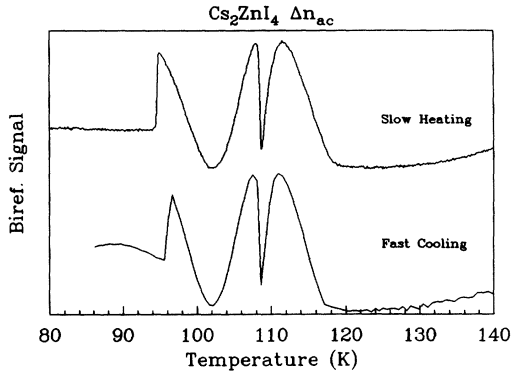

FIG. 7. Lock-in output for fast-heating and slow-cooling runs.

birefringence. In the fast-cooling run, this region shows a large amount of curvature, indicating a changing birefringence. The transmitted intensity measurements also indicate (in the fast-cooling or -heating runs) that there is a large drop in the transmitted intensity below the 94-K transition. Visually, this is seen as diffuse scattering (increasing the total area that the transmitted light subtends, thus lowering the total amount of light striking the power meter detector). This seems to indicate a dynamic process with a relatively long-time constant.

VI. DISCUSSION

As alluded to earlier, Cs_2ZnI_4 probably does not belong to the K_2SeO_4 structural family. The lack of a spontaneous polarization at any temperature is sufficient evidence to rule out the existence of a ferroelectric phase.[6] The NMR spectra of Cs_2ZnI_4 (Ref. 7) also more closely resemble those of Cs_2CdBr_4. This would suggest that one of the lower-temperature phases of Cs_2ZnI_4 should be ferroelastic. In our fast- and slow-cooling cycles, we have seen what appears to be a slow dynamic process in the birefringence and transmitted intensity in at least the lowest-temperature phase. We believe that this process is the formation, growth, and movement of ferroelastic domains. The scattering observed in the transmitted intensity data would then be due to scattering from domain walls.

One other member of the Cs_2CdBr_4 family is Cs_2HgBr_4. In 1981, Plesko *et al.* measured the birefringence of Cs_2HgBr_4.[12] Comparison of our data to Fig. 1 of Plesko *et al.* shows great similarity. Cs_2HgBr_4 has four phase transitions, of which only three are clearly seen in birefringence. The Δn_{ab} birefringence anomalies of Cs_2HgBr_4 are smaller than the anomalies observed in the other two directions, as we have observed in Cs_2ZnI_4. The transitions in Cs_2HgBr_4 are of second, first, second, and first order (from highest temperature to lowest temperature, respectively), again, as they appear to be in Cs_2ZnI_4.

Figure 8(a) shows schematically the phases of Cs_2HgBr_4. Based on the evidence presented here and in Refs. 6 and 7 and assuming the existence of four phase transitions, we believe that Cs_2ZnI_4 will follow a similar phase sequence as shown in Fig. 8(b). If the phase transition at 101 K does not exist, Cs_2ZnI_4 would closely match the phase diagram of Cs_2CdBr_4, which is essentially the same as that of Cs_2HgBr_4 except that the lowest phase transition is missing. In any case it seems clear that Cs_2ZnI_4 belongs to this family of ferroelastic compounds and not to the K_2SeO_4 family of ferroelectrics.

TABLE II. Phase-transition temperatures of Cs_2ZnI_4.

	T_1	T_2	T_3	T_4
This work	119.8 K	109.4 K	101.3 K[a]	94.0 K[b]
Gesi[c]		109.3 K	101.7 K	91.0 K[b]
Aleksandrova *et al.*[d]	118.2 K	107.9 K		95.1 K

[a]Weak transition signature.
[b]Thermal hysteresis was observed at this transition.
[c]Reference 6.
[d]Reference 7.

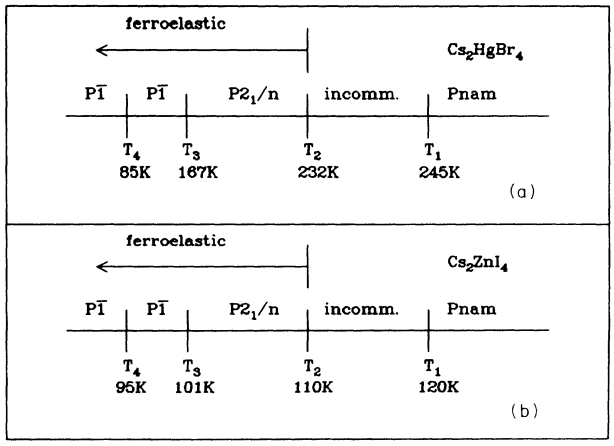

FIG. 8. Proposed phase diagram for Cs_2ZnI_4 compared with the phase diagram for Cs_2HgBr_4.

ACKNOWLEDGMENTS

The authors wish to express their gratitude to Professor R. Kirby for helpful discussions related to this project. This work was supported by the U.S. Army Research Office.

APPENDIX

To analyze the optics of this experiment, we must start with a description of the electric field entering the sample. We can write this as

$$\mathbf{E}_{\text{in}}=E_0[\hat{\mathbf{x}}+Ae^{i\phi}\hat{\mathbf{y}}]\ , \tag{A1}$$

where the oscillatory nature of the field is contained in E_0, ϕ is the phase shift introduced by the compensator (and all other optical elements before the rotating analyzer excluding the sample crystal), and A is the ratio of the maximum values of the x and y components of the field. After passing through the crystal, the modified wave is described by

$$\mathbf{E}_{\text{out}}=E_0[t_x\hat{\mathbf{x}}+t_y Ae^{i[\phi+\delta(T)]}\hat{\mathbf{y}}]\ , \tag{A2}$$

where t_x and t_y are the amplitude transmission coefficients for the x and y directions and $\delta(T)$ is the temperature-dependent phase shift introduced by the change in the sample birefringence.

A convenient technique to analyze the passage of the beam through the rotating analyzer is the Jones matrix formulation.[13] We represent the beam leaving the sample by the column matrix

$$\mathbf{E}_{\text{out}}=E_0\begin{bmatrix} t_x \\ t_y Ae^{i[\phi+\delta(T)]}\end{bmatrix}\ . \tag{A3}$$

The rotating analyzer is represented by the matrix

$$\begin{bmatrix}\cos^2(\omega t+\alpha) & \sin(\omega t+\alpha)\cos(\omega t+\alpha)\\ \sin(\omega t+\alpha)\cos(\omega t+\alpha) & \sin^2(\omega t+\alpha)\end{bmatrix}\ , \tag{A4}$$

where ω is the rotational frequency of the rotating analyzer and α is the phase difference between the rotating-analyzer and crystal axes. This will be abbreviated

$$\begin{bmatrix}C^2 & SC\\ SC & S^2\end{bmatrix}\ . \tag{A5}$$

We can then write the electric field leaving the rotating analyzer as

$$\mathbf{E}_f=E_0\begin{bmatrix}C^2 & SC\\ SC & S^2\end{bmatrix}\begin{bmatrix} t_x \\ t_y Ae^{i[\phi+\delta(T)]}\end{bmatrix}\ . \tag{A6}$$

This expression for the electric field leaving the rotating analyzer reduces to

$$\mathbf{E}_f=E_0[Ct_x+St_y Ae^{i[\phi+\delta(T)]}]\begin{bmatrix}C\\ S\end{bmatrix}\ . \tag{A7}$$

The intensity leaving the rotating analyzer is then

$$I_f=\mathbf{E}_f\cdot\mathbf{E}_f^* \tag{A8}$$

or

$$I_f=I_0[t_x^2\cos^2(\omega t+\alpha)+t_y^2A^2\sin^2(\omega t+\alpha)+t_xt_yA\sin(\omega t+\alpha)\cos(\omega t+\alpha)(e^{i[\phi+\delta(T)]}+e^{-i[\phi+\delta(T)]})]\ . \tag{A9}$$

This reduces to

$$\begin{aligned}I_f=I_0\{&\tfrac{1}{2}(t_x^2+t_y^2A^2)+\tfrac{1}{2}(t_x^2-t_y^2A^2)[\cos(2\omega t)\cos(2\alpha)-\sin(2\omega t)\sin(2\alpha)]\\&+t_xt_yA\cos[\phi+\delta(T)][\sin(2\omega t)\cos(2\alpha)+\cos(2\omega t)\sin(2\alpha)]\}\end{aligned} \tag{A10}$$

or

$$\begin{aligned}I_f=I_0(&\tfrac{1}{2}(t_x^2+t_y^2A^2)+\{t_xt_yA\cos[\phi+\delta(T)]\cos(2\alpha)-\tfrac{1}{2}(t_x^2-t_y^2A^2)\sin(2\alpha)\}\sin(2\omega t)\\&+\{\tfrac{1}{2}(t_x^2-t_y^2A^2)\cos(2\alpha)+t_xt_yA\cos[\phi+\delta(T)]\sin(2\alpha)\}\cos(2\omega t))\ .\end{aligned} \tag{A11}$$

There are three terms to this expression. The first term is a dc term and is independent of the rotating analyzer. The next two terms are proportional to $\sin(2\omega t)$ and $\cos(2\omega t)$ and are thus in phase quadrature with each other. We will call these terms the in-phase and the quadrature components, respectively. We may finally write the intensity leaving the rotating analyzer as

$$I_f=I_{\text{dc}}+I_{\text{in-phase}}+I_{\text{quad}}\ , \tag{A12}$$

where

$$\begin{aligned}I_{\text{dc}}&=\tfrac{1}{2}I_0(t_x^2+t_y^2A^2)\ ,\\ I_{\text{in-phase}}&=I_0\{t_xt_yA\cos[\phi+\delta(T)]\cos(2\alpha)-\tfrac{1}{2}(t_x^2-t_y^2A^2)\sin(2\alpha)\}\sin(2\omega t)\ ,\\ I_{\text{quad}}&=I_0\{\tfrac{1}{2}(t_x^2-t_y^2A^2)\cos(2\alpha)+t_xt_yA\cos[\phi+\delta(T)]\sin(2\alpha)\}\cos(2\omega t)\ .\end{aligned} \tag{A13}$$

[1]H. Z. Cummins, Phys. Rep. **185**, 211 (1990), and references therein.
[2]K. Altermatt, H. Arend, A. Niggli, and W. Petter, Mater. Res. Bull. **14**, 1391 (1979).
[3]S. Plesko, R. Kind, and H. Arend, Ferroelectrics **26**, 703 (1980).
[4]S. Plesko, R. Kind, and H. Arend, Phys. Status Solidi A **61**, 87 (1980).
[5]D. E. Scaife, Aust. J. Chem. **24**, 1315 (1971).
[6]K. Gesi, J. Phys. Soc. Jpn. **50**, 3535 (1981).
[7]I. P. Aleksandrova *et al.*, Ferroelectrics **105**, 177 (1990).
[8]D. P. Billesbach and F. G. Ullman, Phys. Rev. B **43**, 11 432 (1991).
[9]C. Day and V. Day (private communication).
[10]I. G. Wood and A. M. Glazer, J. Appl. Crystallogr. **13**, 217 (1980).
[11]D. P. Billesbach, F. G. Ullman, and J. R. Hardy, Phys. Rev. B **32**, 1532 (1985).
[12]S. Plesko, V. Dvorak, R. Kind, and A. Treindl, Ferroelectrics **36**, 331 (1981).
[13]D. Clarke and J. F. Grainger, *Polarized Light and Optical Measurement* (Pergamon, New York, 1971).